Spatiotemporal Dynamics of Lasers with a Large Fresnel Number

G. Huyet, M. C. Martinoni, J. R. Tredicce, and S. Rica
Institut Non Linéaire de Nice, UMR 129 CNRS-UNSA, 1361 Route des Lucioles, 06560 Valbonne, France
(Received 14 November 1995)

We measure the local intensity and the intensity cross-correlation function of patterns emitted by a CO_2 laser with a Fresnel number around 60 and find evidence of weak turbulence. We show theoretically that the spatiotemporal dynamics of such a laser can be governed by two fields. One leads to a "turbulent" state principally through phase fluctuations, whereas the other yields a periodic modulation in space and time of the intensity. This can explain why the intensity of the laser is locally chaotic but the time-averaged intensity pattern retains the global symmetry of the system.

PACS numbers: 05.45.+b, 42.55.–f, 42.60.Mi, 47.20.Ky

Spatially extended dissipative systems have been the subject of intensive studies during the last 30 years [1]. Pattern formation in lasers has been observed since their discovery [2], but has recently regained interest within the development of nonlinear dynamics [3]. Experimental and theoretical studies of spatiotemporal structures have been most successful in the cases in which there is a low Fresnel number [4,5]. Indeed, the richness of the dynamics of few modes yields a quantity of experimental and theoretical results. On the other hand, it is difficult to find experimental results in the literature for lasers operating at high Fresnel number. Previous works showed only the existence of relatively complex patterns in the time-averaged intensity distribution [6] without indications about the degree of complexity and/or the physical origin of such particular spatial structures.

In this paper, we present detailed experimental measurements of the dynamical behavior of a similar laser that indicate strong differences from recent theoretical predications. We find neither vortices nor grain boundaries. Consequently, we provide an alternative interpretation and approximation to the standard Maxwell-Bloch model that describes the evolution and characteristics of patterns observed in our experiment. Our theoretical results show that the formation of structures is controlled by two generic spatiotemporal instabilities. The first is a long-wavelength instability that is related to the phase fluctuations of the field. It is described by a Kuramoto-Shivasinsky (KS) type equation [7]. The second is a short-wavelength instability of the field amplitude. It corresponds to a Hopf bifurcation selecting a well-defined wavelength and it is described by a complex Swift-Hohenberg (CSH) equation [8]. As a result, the laser intensity presents a turbulent behavior, at a short time scale, due to the dynamics of KS. However, the time average patterns display the typically organized structure of the CSH equation. This picture is an example of a turbulent field which recovers symmetry on average. Similar phenomena have been observed in recent experiments in hydrodynamics in which the pattern is very irregular in space and time, but the average time pattern recovers the symmetry of the boundary [9].

The experimental setup we use is analogous to the one described in Ref. [6]. An example of the time-averaged transverse pattern emitted by a Fabry-Pérot CO_2 laser with an intracavity lens resulting in a Fresnel number (F_r) of 60 is shown in Fig. 1(a). This appears as an ordered structure of concentric rings when the laser is perfectly aligned. If the system is not perfectly aligned we observe structures such as squares, or even more complex patterns. However, all the measurements described below apply qualitatively to any observed pattern. These patterns seem to show a relatively large number of points where we could assume the presence of topological defects [10]. However, we must take into account the nonlinear response of the plate which may have led to confusion over evidence for defects [6]. But, if we measure the intensity profile along a diameter with a HgCdTe detector, we note that the intensity is much larger than zero at every spatial point and time in the region of interest. The temporal oscillations, which represent about 10% of the dc signal in the electric field amplitude, are much greater than the noise. Thus the experimental intensity distribution of Fig. 1 can be interpreted as an almost constant intensity modulated in space by a periodic structure and weakly modulated in time. For low F_r the periodic temporal oscillations are at frequencies that vary from 400 kHz to 2 MHz. As F_r

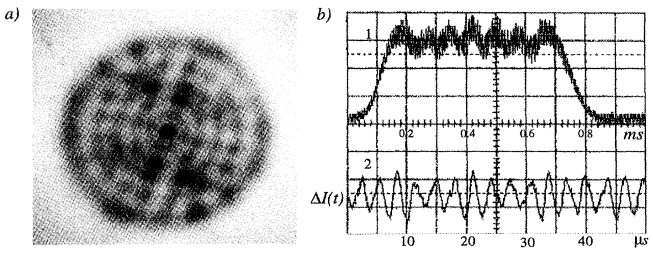

FIG. 1. (a) Average intensity pattern observed on an infrared image plate. (b1) Intensity vs transverse coordinate measured with a rotating mirror which deflects the beam onto a fast HgCdTe detector. The pattern is here composed of four concentric rings. The detector linear size is 500 of the pattern width. (b2) ac component of the intensity at a point.

0031-9007/95/75(22)/4027(4)$06.00

is increased, the oscillations at high frequency disappear while a large peak develops in the power spectrum near 150 kHz. This frequency is of the order of magnitude of the relaxation oscillation frequency when our CO_2 laser operates single mode.

Moreover, we measured the spatial correlation function to distinguish the spatiotemporal behavior reported in this Letter from low-dimensional chaos as was done for a photorefractive oscillator [11]. We used two detectors to calculate the spatial correlation of the pattern. The first detector measures the intensity at the center of the pattern while the second one measures the intensity of the beam deflected by a rotating mirror. As the rotating mirror moves very slowly, we can measure the maximum over time of the cross-correlation function between signals from two different points. We take a normalization such that, if the signals are perfectly correlated at any delay time, then the value is 1; if they are uncorrelated the value is 0. We have measured this spatial correlation for different patterns as the Fresnel number is increased. For patterns which have periodic oscillations (low pump or low Fresnel number), the spatial correlation function is equal to 1 everywhere. When the complexity is increased, the temporal behavior of the intensity becomes chaotic with a small number of modes. The spatial correlation is no longer equal to 1 everywhere, but decreases with oscillations. But in the case of high Fresnel number, the shape of the correlation function changes dramatically to that found in Fig. 2(b), with a narrow peak. Experimentally we find that the correlation length (width of the peak) is about $\frac{1}{6}$ of the width pattern.

This behavior is not predicted by the approximate theoretical approaches used up to now in optics. Previous work based on the Ginzburg-Landau equation [10] for negative detuning (and its extension for positive detuning [12]), and for class B lasers [13], when restricted to an almost infinite Fresnel number near the lasing threshold, predicted defects. One reason for the disagreement between previous theories and our experiment is the finite size of real experimental systems, which gives a small

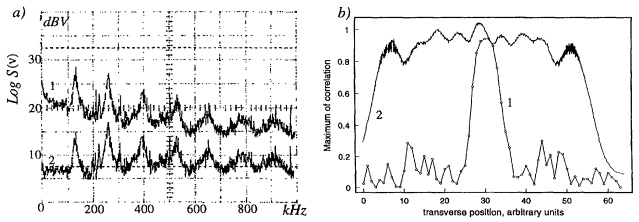

FIG. 2. (a1) The power spectrum, averaged over 200 acquisitions time, of the local intensity. (a2) The same power spectrum minus the power spectrum of the noise. There is a broadband peak near 150 kHz and its harmonics. (b1) Plot of the normalized spatial correlation function. (b2) average intensity measured from the rotating mirror, with which we can compare the correlation length with the radius of the beam.

Fresnel number at threshold. However, theories that take into account the finite size predict transverse standing waves near the threshold [14] that we do not find in the experiment. Hence, none of the previous theoretical approaches explains our simple direct observation of the absence of defects and almost constant intensity in space with a weak spatiotemporal modulation of the intensity.

The starting point for our theoretical interpretation of these experimental results is the Maxwell-Bloch (MB) equations in a dimensionless form, for the slowly varying envelopes of electric field $E(\mathbf{x},t)[\mathbf{x} = (x,y)]$, polarization $P(\mathbf{x},t)$, and population inversion $D(\mathbf{x},t)$:

$$\partial_t E = -\kappa[(1 - i\delta) - i\tfrac{a}{2}\nabla^2]E - \kappa CP; \quad (1a)$$

$$\partial_t P = -\gamma_\perp[DE + (1 + i\delta)P]; \quad (1b)$$

$$\partial_t D = -\gamma_\parallel[-\tfrac{1}{2}(E^*P + EP^*) + D - 1]; \quad (1c)$$

where κ, $\gamma_\perp$, and $\gamma_\parallel$ are the decay rates for E, P, and D, respectively. For modeling a CO_2 laser we take $\gamma_\perp/\kappa \approx 5$, $\gamma_\parallel/\kappa \approx 0.01$, and $\kappa \approx 2 \times 10^7\ s^{-1}$. The pump strength is denoted by C (between 2 and 3 in the experiment, where $C = 1$ at threshold), δ is the cavity detuning; a is inversely proportional to the Fresnel number; and ∇^2 is the transverse Laplacian.

To explain the experimental profile found in the center of Fig. 1(b) by an approximate solution of the MB equations, we consider a homogeneous solution where $|E_0|^2 = C - (1 + \delta^2)$. The phase of E_0 is not fixed, since the MB equations (1) are invariant under a global phase change $E \rightarrow Ee^{i\phi_0}$, together with $P \rightarrow Pe^{i\phi_0}$, for ϕ_0 an arbitrary real number.

We perform a linear stability analysis of homogeneous solution in Fourier space. It appears that analytic solutions are not possible, yet we note that we have the following.

(i) One real eigenvalue, associated with the phase invariance of (1), given by (near $k \approx 0$)

$$\lambda_0(k) = k_0^2 k^2 - \frac{c_0}{2}k^4 + O(k^6), \quad (2)$$

where $k_0^2 \approx \kappa\delta(a/2)$ and $c_0 \approx \kappa[C(1 + \delta^2)a^2]/2|E_0|^2$. If $\delta > 0$, this phase mode is always unstable since $\lambda_0(k) > 0$ for long-wavelength perturbations. This global phase is an important variable for the dynamics and it obeys a KS type equation.

(ii) If $\gamma_\parallel \ll \kappa$, $\gamma_\perp$ (for class B lasers such as CO_2 or Nd:YAG lasers [15]), there is a spatially extended Hopf bifurcation with a well-defined wave number q_0 (q_0 is much larger than k_0). Thus we have two complex conjugate eigenvalues given by the following Taylor expansion around q_0^2:

$$\lambda_1(k) = (\mu + i\Omega) - i\upsilon(q_0^2 - k^2) - \alpha(q_0^2 - k^2)^2 + \cdots, \quad (3)$$

where μ, Ω, and υ are real coefficients while α is a complex quantity. Thus in the neighborhood of the bifurcation the dynamics is governed by a complex

field which obeys a CSH equation. The frequency Ω of the Hopf bifurcation is roughly given by $\Omega \approx \sqrt{2\kappa\gamma_\parallel|E_0|^2/(1+\delta^2)}$, which is obviously the relaxation oscillation frequency for all class B single mode lasers. This Hopf frequency will be a characteristic of the spatiotemporal dynamics of class B lasers.

(iii) The last two complex eigenvalues have very large negative real parts and they are roughly given by $\lambda_2^{\pm} \approx -\gamma_\perp(1 \pm i\delta)$. Thus the associated eigenmodes do not play a relevant role in the dynamics (except for class C lasers).

Therefore the dynamics of a class B laser originating from a homogeneous nonzero state of the field will be governed by a real field ϕ and a complex one A. The linear dynamics is given (in Fourier space) by $\partial_t\phi_k = \lambda_0(k)\phi_k$ and $\partial_t A_k = \lambda_1(k)A_k$. The physical variables are functions of ϕ and A. Taking the electric field amplitude $|E|$ as an example, we have

$$\frac{|E|}{|E_0|} \approx 1 - \frac{a}{4}\left(1 + \frac{1+\delta^2}{|E_0|^2}\right)\nabla^2\phi - i(Ae^{i\Omega t} - A^* e^{-i\Omega t}) + O[|A|^2, (\nabla\phi)^2]. \tag{4}$$

The linearized problem and symmetry arguments (invariance under the transformation $A \to Ae^{i\psi_0}$ and $\phi \to \phi + \phi_0$) can be used to obtain directly the general form of the equations:

$$\partial_t\phi = -k_0^2\nabla^2\phi - \frac{c_0}{2}\nabla^4\phi + c_1(\nabla\phi)^2 + c_2|A|^2; \tag{5a}$$

$$\partial_t A = \mu A - iv(q_0^2 + \nabla^2)A - \alpha(q_0^2 + \nabla^2)^2 A - [\beta_1|A|^2 + \beta_2(\nabla\phi)^2]A + \beta_3\nabla\phi\cdot\nabla A; \tag{5b}$$

where c_1 and c_2 are real while β_1, β_2, and β_3 are complex. The nonlinear terms ensure the saturation. The phase equation (5a) describes well the long-wavelength behavior in the transverse direction of any laser, since it is directly related to the phase invariance of the electromagnetic field.

Then the general behavior of the electromagnetic field depends on the signs of k_0^2 and μ. Four different cases could occur:

(i) If $k_0^2 < 0$ and $\mu < 0$ (i.e., for lasers with $\delta < 0$), the steady-state solution is stable.

(ii) If $k_0^2 < 0$ and $\mu > 0$ Eq. (5a) is purely diffusive and $\nabla\phi$ goes to zero. Equation (5b) creates a periodic structure which oscillates in time. It is important to note that $k_0^2 < 0$ implies that the detuning $\delta < 0$ which is precisely the case where the longitudinal monomode approximation is usually not valid since the transversal modes of a neighboring longitudinal mode enter the gain curve in lasers with a large Fresnel number.

(iii) If $k_0^2 > 0$ and $\mu < 0$, the KS equation becomes very irregular in space and time. The observed state is the so-called "phase turbulence" [7,16]. However, the temporal mean values [$\langle\nabla^2\phi\rangle$ and $\langle(\nabla\phi)^2\rangle$] become constant in space (the former is zero). Consequently, the signal $|E(\mathbf{x},t)|^2$ [given by Eq. (4)] displays a complex behavior in time, but the time averaged pattern appears homogeneous in space.

(iv) If $k_0^2 > 0$ and $\mu > 0$ ($\delta > \delta_c$)—the most interesting case—then the two instabilities occur. The phase ϕ has a dynamics analogous to the numerical simulations of KS. The instability associated with the CSH creates a periodic structure in the amplitude of the field. This structure oscillates in time at Ω (and harmonics), but its lamellar characteristic structure is dismantled by the dynamical evolution of ϕ. As a consequence, A shows a complex spatiotemporal behavior. If we seek a stationary solution of (5b) in the form $A = |A|e^{iq_0x}$ (in which all the coefficients are taken as real and $\beta_3 = 0$) we find that A depends on the "stochastic variable" ϕ as ($\beta_2^{(r)} \equiv \mathrm{Re}\beta_2$)

$$|A|^2 \sim \mu - \beta_2^{(r)}(\nabla\phi)^2. \tag{6}$$

The instantaneous value of $A = |A|e^{iq_0x}$ looks more disorganized than the mean value $\langle|A|e^{iq_0x}\rangle$ because of its explicit dependence on the turbulent field $\nabla\phi$. The mean value instead recovers the periodic structure

$$\langle A\rangle \sim \left(\sqrt{\mu} - \frac{\beta_2^{(r)}}{2\sqrt{\mu}}\langle(\nabla\phi)^2\rangle\right)e^{iq_0x} \sim e^{iq_0x},$$

since $\langle(\nabla\phi)^2\rangle$ is constant. We illustrate our analytical arguments in Fig. 3 through a direct numerical simulation of the coupled equations (5a) and (5b).

A heuristic explanation of measurements of the cross-correlation function can be given in terms of the phase dynamics as the Fresnel number is increased. The number of degrees of freedom of the KS equation grows as $N_{KS} \sim (Rk_m)^2$, where R is the transverse radius of the

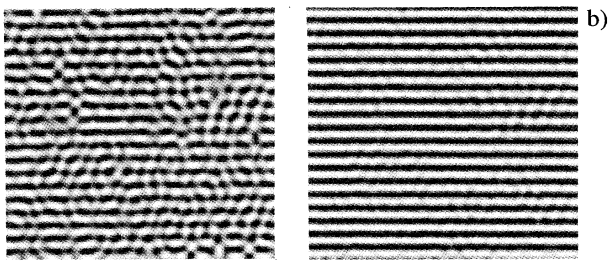

FIG. 3. Numerical simulations of the model with all the coefficients real. (a) The instantaneous value of ReA. The initial conditions are rolls parallel to the x axis. (b) The temporal average $\langle A\rangle$.

laser beam in the cavity. Moreover, N_{KS} is proportional to the Fresnel number (F_r) of the laser cavity. For small F_r, such that $N_{KS} \approx 1$, the KS equation leads to low-dimensional chaos. In this case, the spatial cross-correlation functions decay slowly, since they are only determined, typically, by the long range order as in crystals. However, for a large Fresnel number, the solutions of the KS equations become turbulent and the correlation function is screened by a factor $e^{-\Delta x/\lambda_c}$ (Δx the spatial separation of two points), with $\lambda_c \sim k_m^{-1}$, which depends on the Fresnel number as $\lambda_c/R \sim 1/\sqrt{F_r}$. For relatively large Fresnel number, the correlation length decreases, becoming much smaller than R. The resulting state may be called (weak) optical turbulence. The case (iv), for which the two instabilities occur, may explain the spatiotemporal behavior experimentally observed. We observe complex spatiotemporal oscillations around the relaxation frequency. Thus, in the framework of the model, we are in the case (iv), where we can explain the oscillations and the losses of spatial and temporal correlations. However, one may verify experimentally phase turbulence in a laser with measurements of the phase of the electromagnetic field. In this case we should see that the phase fluctuations are coupled with amplitude instabilities.

In conclusion, we have shown experimental evidence of the absence of "defects" in the transverse intensity pattern of a laser with $F_r \approx 60$. We show the appearance of chaotic oscillations centered around the relaxation oscillation frequency, and the loss of spatial correlation. We also show that these results can be explained as a characteristic of the usual Maxwell-Bloch equations when two "fields" are involved in the dynamics, one a scalar field obeying the Kuramoto-Shivasinsky equation and the other a complex field which obeys a Swift-Hohenberg equation.

Finally, we acknowledge N. B. Abraham for his constant interest and useful advice. It is a pleasure to thank F. T. Arecchi, P. Coullet, Y. Pomeau, A. Pumir, and E. Tirapegui for stimulating discussions, and J. Clark for her help. We also acknowledge L. Hoffer for providing acquisition software.

[1] P. Manneville, *Dissipative Structures and Weak Turbulence* (Academic Press, New York, 1990); M. C. Cross and P. C. Hohenberg, Rev. Mod. Phys. **65**, 851 (1993).
[2] W. W. Rigrod, Appl. Phys. Lett. **2**, 51 (1963).
[3] Special Issue on Transverse Effects in Optical Systems, edited by N. B. Abraham and W. Firth [J. Opt. Soc. Am. B **7**, 951–1373 (1990)].
[4] C. Green, G. B. Mindlin, E. J. D'Angelo, H. G. Solari, and J. R. Tredicce, Phys. Rev. Lett. **65**, 3124 (1990).
[5] E. J. D'Angelo, E. Izaguirre, G. B. Mindlin, G. Huyet, L. Gil, and J. R. Tredicce, Phys. Rev. Lett. **68**, 3702 (1992).
[6] D. Dangoise, D. Hennequin, C. Lepers, E. Louvergneaux, and P. Glorieux, Phys. Rev. A **46**, 5955 (1992).
[7] Y. Kuramoto and T. Tsuzuki, Prog. Theor. Phys. **55**, 356 (1976); G. I. Shivasinsky, Acta Astronaut. **4**, 1177 (1977); see also Y. Kuramoto, *Chemical Oscillations, Waves and Turbulence* (Springer, New York, 1984). For lasers the KS equation has been introduced by R. Lefever, L. A. Lugiato, W. Kaige, N. B. Abraham, and P. Mandel, Phys. Lett. A **135**, 254 (1989).
[8] J. Swift and P. C. Hohenberg, Phys. Rev. A **15**, 319 (1977).
[9] B. J. Gluckman, P. Marcq, J. Bridger, and J. P. Gollub, Phys. Rev. Lett. **71**, 2034 (1993); L. Ning, Y. Hu, R. Ecke, and G. Ahlers, Phys. Rev. Lett. **71**, 2216 (1993).
[10] P. Coullet, L. Gil, and F. Rocca, Opt. Commun. **73**, 403 (1989).
[11] S. R. Liu and G. Indebetouw, J. Opt. Soc. Am. B **9**, 1507 (1992).
[12] A. C. Newell, in *Spatio-Temporal Patterns in Nonequilibrium Complex Systems,* edited by P. E. Gladis and P. Palffy-Muhoray (Addison-Wesley, Reading, MA, 1993), Vol. XXI.
[13] J. Lega, J. V. Moloney, and A. C. Newell, Phys. Rev. Lett. **73**, 2978 (1994).
[14] K. Staliunas and C. O. Weiss, Physica (Amsterdam) **81D**, 79 (1995); G. K. Harkness, W. J. Firth, J. B. Geddes, J. V. Moloney, and E. M. Wright, Phys. Rev. A **50**, 4310 (1994).
[15] F. T. Arecchi, G. L. Lippi, G. P. Puccioni, and J. R. Tredicce, Opt. Commun. **51**, 308 (1984).
[16] P. Manneville, Phys. Lett. A **84**, 129 (1981); Y. Pomeau, A. Pumir, and P. Pelce, J. Stat. Phys. **37**, 39 (1984); G. I. Shivasinsky, Annu. Rev. Fluid Mech. **15**, 179 (1983).

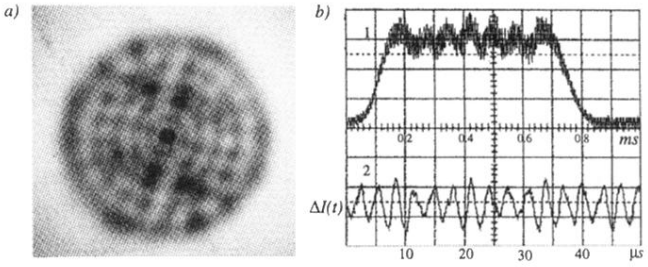

FIG. 1. (a) Average intensity pattern observed on an infrared image plate. (b1) Intensity vs transverse coordinate measured with a rotating mirror which deflects the beam onto a fast HgCdTe detector. The pattern is here composed of four concentric rings. The detector linear size is 500 of the pattern width. (b2) ac component of the intensity at a point.

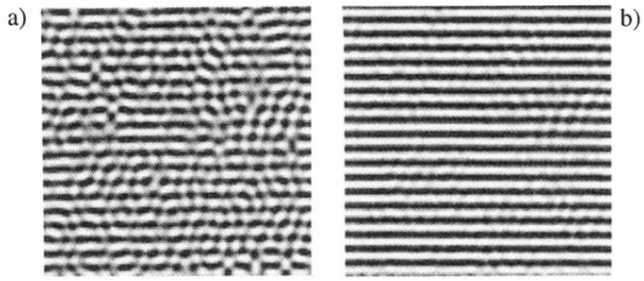

FIG. 3. Numerical simulations of the model with all the coefficients real. (a) The instantaneous value of ReA. The initial conditions are rolls parallel to the x axis. (b) The temporal average $\langle A \rangle$.